Surface-Grafted Stimuli-Responsive Block Copolymer Brushes for the Thermo-, Photo- and pH-Sensitive Release of Dye Molecules

ARTICLE *in* MACROMOLECULES · SEPTEMBER 2011

Impact Factor: 5.8 · DOI: 10.1021/ma2010102

4 AUTHORS, INCLUDING:

Surjith Kumar
University of Alberta
10 PUBLICATIONS **262** CITATIONS
SEE PROFILE

Yves Dory
Université de Sherbrooke
98 PUBLICATIONS **1,041** CITATIONS
SEE PROFILE

Macromolecules

ARTICLE

pubs.acs.org/Macromolecules

Surface-Grafted Stimuli-Responsive Block Copolymer Brushes for the Thermo-, Photo- and pH-Sensitive Release of Dye Molecules

Surjith Kumar,[†,‡] Yves L. Dory,[*,†] Martin Lepage,[*,‡] and Yue Zhao[*,†]

[†]Département de chimie, Université de Sherbrooke, Sherbrooke, Québec J1K 2R1, Canada

[‡]Département de médecine nucléaire et de radiobiologie and Centre d'imagerie moléculaire de Sherbrooke, Université de Sherbrooke, Sherbrooke, Québec J1H 5N4, Canada

Supporting Information

ABSTRACT: We present a general approach for using surface-grafted stimuli-responsive diblock copolymer brushes as stimuli-sensitive and controllable release systems. Surface-initiated ATRP was used to grow sequentially a first block serving as an inner reservoir for loading and a second block that acts as a stimuli-responsive outer layer controlling the closure or opening of the brush in water. We show that the release kinetics of loaded model dyes (hydrophobic or hydrophilic) could be controlled by the second block switchable between the collapsed and extended brush chain states in response to temperature or pH change or exposure to light. On the one hand, diblock copolymer brushes of polystyrene-*b*-poly(*N*-isopropylacrylamide) (PS-*b*-PNIPAM) and poly(*N*,*N*′-dimethylacrylamide)-*b*-poly(*N*-isopropylacrylamide) (PDMA-*b*-PNIPAM) were synthesized to demonstrate the thermosensitive release of dyes based on the LCST-determined solubility switching between swollen and collapsed PNIPAM chains. On the other hand, a diblock copolymer brush of polystyrene-*b*-poly(4,5-dimethoxy-2-nitrobenzyl methacrylate) (PS-*b*-PNBA) was designed to investigate the possibility of tuning the dye release kinetics with light. The photocontrol was achieved by controlling the photocleavage degree of photolabile *o*-nitrobenzyl groups, which determines the number of hydrophilic methacrylic acid (MA) groups in the outer layer. Moreover, complete photocleavage of *o*-nitrobenzyl groups converted the photosensitive PS-*b*-PNBA brush into a pH-sensitive PS-*b*-PMA brush with which pH-dependent dye release was observed due to the water solubility switching of PMA chains with protonated or ionized carboxylic acid groups. The interest, the versatility, and the generality of the approach were demonstrated in this study with three different stimuli, namely, temperature, pH, and light.

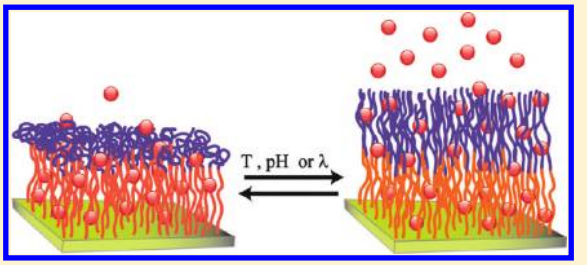

1. INTRODUCTION

Polymer-based delivery systems, particularly with respect to targeted biomedical applications, such as controllable drug release, have attracted much attention in polymer chemistry, pharmaceutics, and biomaterials science.[1] As such, several platforms have been exploited for these purposes, including the fabrication of polymer−protein[2] and polymer−drug conjugates,[3] micelles,[4] vesicles,[5] and dendrimers.[6] Although the controlled release from three-dimensional (3D) particles remains the predominant drug delivery method, interest has increased in surface-based delivery systems for the controlled release of therapeutic molecules.[7]

At present, there is an increasing research effort focused on stimuli-responsive thin films and coatings that combine a wide range of fundamental scientific and commercial objectives.[8] These smart polymer films have been proposed for various applications, including drug delivery systems,[9] liquid crystal command layers,[10] antireflection coatings,[11] switchable friction,[12] and membrane permeation mechanisms.[13] While techniques such as spin-coating, self-assembled monolayers, and the Langmuir−Blodgett method have been employed for the macromolecular assembly of ultrathin films, other coating methods have gained much popularity, most notably the layer-by-layer (LbL) and polymer brush techniques. The LbL self-assembly of macromolecules can be performed on a variety of substrate types and shapes with precisely controlled nanometer dimensions.[14] Using LbL-assembled films, several groups have demonstrated successfully the delivery of highly charged biomacromolecules and the uptake and release of small model drug compounds.[15,16] Hydrolytically degradable LbL films have been demonstrated for tunable drug release;[17] drug-conjugated polyelectrolyte prodrugs were added to the components of the films, and cell viability was assayed.[18] Recently, we and other groups have reported the fabrication of LbL films of amphiphilic block copolymer micelles where hydrophobic compounds could be loaded into the micelle core.[19] However, the LbL techniques are generally limited to the use of charge-opposing polyelectrolytes, which are not generally thought to be good candidates for lipophilic drug-loading. Thus, development of thin film-based delivery systems for hydrophobic compounds is of interest.

Received: May 3, 2011
Revised: August 17, 2011
Published: August 29, 2011

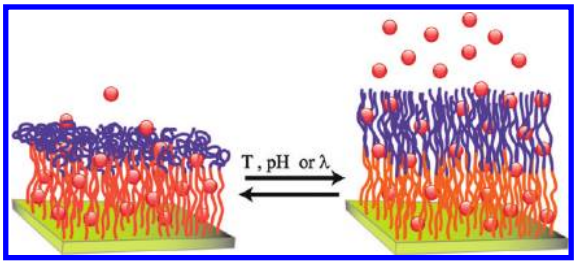

Figure 1. Schematic illustration of surface-grafted diblock copolymer brushes of which the top layer can exhibit switching between collapsed and extended chains in response to temperature change, pH change, or exposure to light.

Surface-initiated polymer brushes may represent an alternative system that overcomes this limitation. An appealing feature of polymer brushes is their high degree of synthetic flexibility and mechanical and chemical robustness.[20] For the preparation of polymer brushes via the grafting from technique, controlled radical polymerizations (CRP) have offered many benefits, namely, control over the thickness of the brush, uniformity of the brush surface, and the ability to produce brushes with complex architectures by making use of the large body of knowledge on polymer synthesis. These advantages have made CRP the technique of choice in the preparation of well-defined polymer brushes. Arguably, the most common CRP technique currently used is atom transfer radical polymerization (ATRP).[21] Because of the development of surface-initiated living polymerization methods, numerous reports have appeared in recent years regarding the synthesis of stimuli-responsive polymer brushes, which have potential applications in a broad range of fields, including colloid stabilization, nonbiofouling surfaces, membranes, sensors for temperature, ions, and pH.[22]

In this article, we describe a general approach for developing stimuli-responsive block copolymer (BCP) brushes that may have interest for controlled delivery applications. As schematized in Figure 1, surface-initiated ATRP can be used to graft a first polymer to form an inner layer that acts primarily as a reservoir for guest molecules; then, a second polymer, which is stimuli-responsive, can be grown through chain extension to form the outer layer. The idea is to use the switchable water solubility of the outer layer to close or open the brushes (i.e., the outer chain is collapsed or swelled) in response to a stimulus that may be either a temperature change, a pH change, or exposure to light. Such stimuli-induced switching can be used to control the release kinetics of the entrapped guest molecules. For instance, if the top layer is a polymer exhibiting a lower critical solution temperature (LCST), it should swell at T < LCST, thus opening channels within the brush as a result of the water solubility. This favors the release. In contrast, the top layer should collapse at T > LCST, contracting the polymer chains and thereby restraining the flow of loaded molecules. The same rationale can be applied to design BCP brushes of which the top layer has pH- and light-switchable water solubility. In the present study, we have synthesized several BCP brushes that are either thermo-, photo-, or pH-sensitive and investigated the effect of their solubility change in response to these stimuli on the release kinetics of entrapped model dye molecules. The results show the potential for developing surface-grafted BCP brushes as a platform for controlled delivery applications.

2. EXPERIMENTAL SECTION

Details on the synthesis of BCP brushes using surface-initiated ATRP as well as their characterizations are given in the Supporting Information.

3. RESULTS AND DISCUSSION

3.1. Synthesis and Characterization. The chemical structures of the stimuli-responsive diblock copolymer brushes synthesized in this study are shown in Figure 2 together with the model dyes utilized for the release test, which were nile red (NR, hydrophobic) and 1,3,6,8-pyrenetetrasulfonic acid tetrasodium salt (PSA, hydrophilic). On the one hand, the BCP brushes PS-*b*-PNIPAM and PDMA-*b*-PNIPAM were built from polystyrene (PS) and poly(*N*-isopropylacrylamide) (PNIPAM), and from poly(*N*,*N*-dimethylacrylamide) (PDMA) and PNIPAM, respectively. They both have a thermosensitive top layer of PNIPAM with a LCST at approximately 32 °C[23] but differ in the inner block, with PS favoring the solubilization of NR and PDMA for the loading of PSA. On the other hand, the diblock brush PS-*b*-PNBA has a photosensitive top layer of poly(*o*-nitrobenzyl methacrylate) (PNBA) bearing photolabil *o*-nitrobenzyl side groups. PNBA is hydrophobic, but upon exposure to UV light, the cleavage of *o*-nitrobenzyl groups converts PNBA into hydrophilic poly(methacrylic acid)[24] (PMA), inducing, thereby, the transition from the collapsed to swelled state of the top layer. With this photochemical reaction, the photoinduced change is not reversible. Interestingly, the resulting PS-*b*-PMA is pH-sensitive with which a reversible pH change across the pK_a of PMA (6−7)[25] can trigger a reversible transition between collapsed chains (with protonated acid groups, insoluble in water) and swelled chains (with ionized acid groups, soluble in water). Therefore, the synthesized BCP brushes allowed us to investigate the effect of thermo-, photo-, and pH-induced transitions of the brush on the release of NR or PSA. Also schematically illustrated in Figure 2 is the setup used to monitor the release kinetics of dye molecules entrapped in the BCP brush. Basically, a quartz cell was closed with a dialysis cap and filled with water with a total volume of ∼4 mL (the same solution in the cuvette and the cap); the substrate (silicon wafer or quartz plate) containing a BCP brush and loaded dye molecules (see the Supporting Information for details on the loading) was then immersed in the cap so that dye molecules released from the brush could diffuse through the dialysis membrane (cutoff MW 2000 Da) and be detected by measuring the fluorescence intensity of dye molecules in the bulk solution.

The synthesis of our BCP brushes was carried out by using surface-initiated ATRP, which is a method used to graft BCP brushes with controlled architecture and defined surface morphology.[26,27] First, 3-aminopropyl triethoxy silane (APTES) was immobilized onto a cleaned silicon wafer or quartz surface by a self-assembled process; it was then reacted with 2-bromo-2-methylpropionyl bromide to yield a Br-functionalized initiator surface. For the brushes of PS-*b*-PNIPAM and PDMA-*b*-PNIPAM, PS was grafted to the initiator-functionalized surfaces via ATRP using a styrene/toluene solution (3:1, v:v) at 130 °C for 3 h, producing tethered PS chains in the form of ∼70 nm thick brushes. For the PDMA brush, it was obtained by ATRP of DMA in water at 80 °C for 8 h, generating ∼40 nm thick layers on the substrate. NIPAM was finally polymerized on the PS- or PDMA-modified substrates to yield ∼187 and 167 nm thick PS-*b*-PNIPAM and PDMA-*b*-PNIPAM brushes, respectively. For

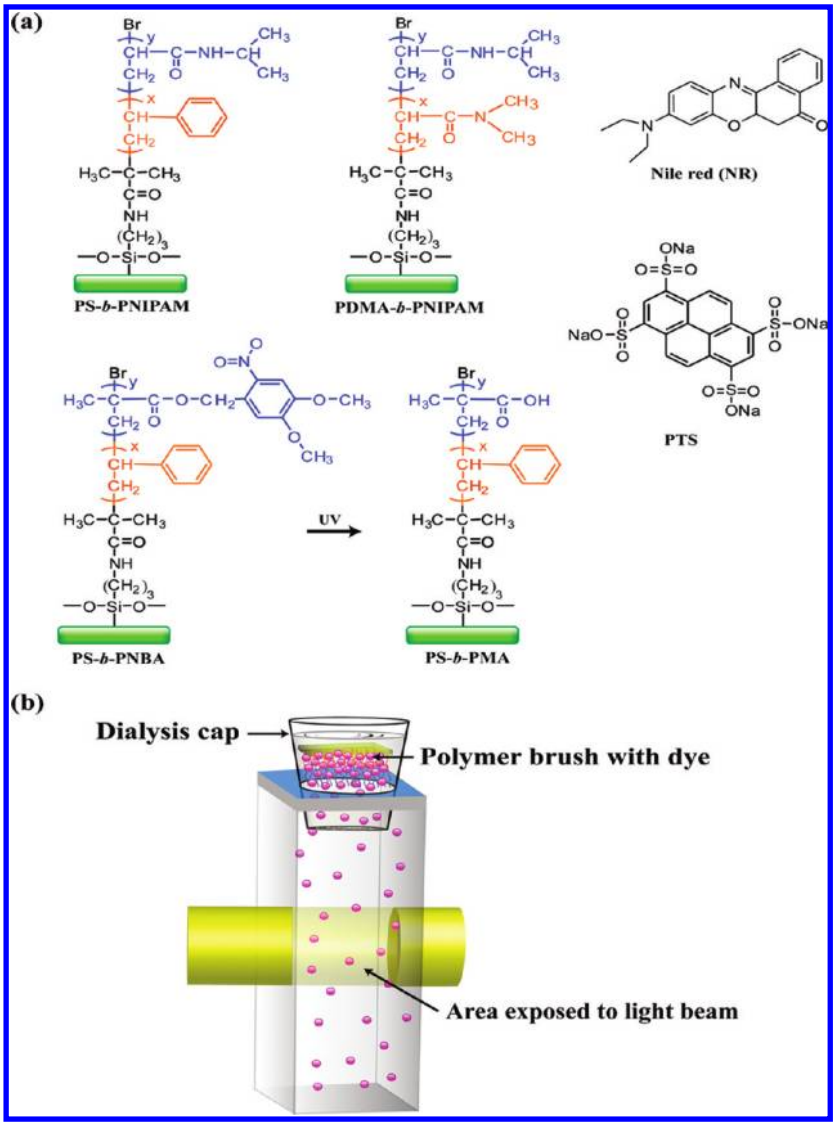

Figure 2. (a) Chemical structures of the diblock copolymer brushes investigated and the fluorescence dyes used in this study. (b) Schematic illustration of the setup used to monitor the dye release from diblock copolymer brushes.

photosensitive PS-*b*-PNBA brushes on silicate substrates, the synthesis was accomplished by a sequential process involving ATRP of styrene as previously described, followed by polymerization of 4,5-dimethoxy-2-nitrobenzyl methacrylate (NBA) in dry dimethyl sulfoxide (DMSO) at 90 °C for 24 h.

All BCP brushes were characterized by X-ray photoelectron spectroscopy (XPS), atomic force microscopy (AFM), and water contact angle measurements. The results indicate successful grafting of the BCP brushes in all cases (see the Supporting Information). For instance, the advancing contact angle increased from 81 ± 2° for the initiator surface to 91 ± 4° after growth of the hydrophobic PS brush, but it dropped to 17 ± 3° when the hydrophilic PNIPAM brush was grafted. In the case of PDMA-*b*-PNIPAM on a silicon wafer, this angle was 30 ± 1° with PDMA and changed to 21 ± 2° after the growth of the PNIPAM block on top. The XPS analysis confirmed the presence of bromine (Br 3d) on the surface with an immobilized ATRP initiator. After the grafting of the polymers, the appearance of the C1s binding energy at ∼228 eV in the XPS high-resolution scan confirmed that polymer brushes were immobilized on the silicon wafers. The sampling depth of the XPS experiments was about 5−10 nm, depending on the core level binding energy and takeoff angle. The polymer brushes were also examined by AFM (1 μm × 1 μm) in tapping mode. Examination of the brush surface morphologies revealed the formation of a compact layer, with a growing granular structure that indicated film thickening. The root-mean-square (rms) surface roughness of the PS homopolymer brush was ∼2 nm with a thickness of ∼70 nm, whereas a larger roughness and thickness of ∼3.5 and 185 nm, respectively, were estimated for the PS-*b*-PNIPAM brush. The rms surface roughness of the PDMA homopolymer and PDMA-*b*-PNIPAM block copolymer brushes was ∼0.7 and ∼2.7 nm, respectively. Average PDMA and PDMA-*b*-PNIPAM brush thicknesses were estimated to be 40 and 127 nm, respectively. Additionally, the average thickness of PS-*b*-PNBA was ∼93 nm, with an rms roughness of ∼2.8 nm.

3.2. Thermosensitive BCP Brush and Dye Release. A PS-*b*-PNIPAM brush with a hydrophobic inner layer was used for the loading and release experiment of NR, while PDMA-*b*-PNIPAM with a hydrophilic inner layer was used for the experiment with

dx.doi.org/10.1021/ma2010102 |*Macromolecules* 2011, 44, 7385–7393

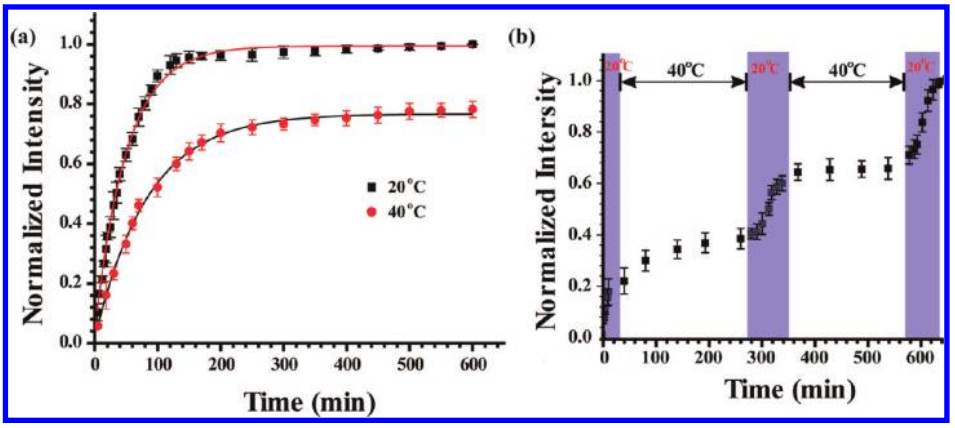

Figure 3. (a) Changes in normalized fluorescence emission intensity of Nile Red (λ_{ex} = 640 nm) over time showing the dye release kinetics from the PS-*b*-PNIPAM brush at two different temperatures. (b) Dye release profile recorded by switching the solution temperature between 20 and 40 °C.

PTS (Figure 2). In a typical dye-loading experiment, the polymer brush was immersed in a dye solution (0.5 mg mL^{-1}, THF with NR and water with PTS) at room temperature (below the LCST of the top PNIPAM layer), where the BCP brush was in the soluble, swelling state. After the impregnation of dye molecules reached a steady state (equilibrium), the film was taken out of the dye solution and dipped in water at 40 °C (above the LCST) to allow the top PNIPAM layer to collapse and thus entrap the dye. This was followd by rinsing the film with 40 °C water three times to remove dye molecules remaining on the film surface. Afterward, using the setup described in Figure 2b, the substrate containing the dye-loaded BCP brush could be placed in a dialysis cap integrated with a quartz cuvette filled with ~4 mL of water thermostated at a given temperature by a temperature-controlled sample holder, and the release of dye molecules diffusing across the membrane was monitored by recording the change in the fluorescence emission intensity of the dye. All measurements were repeated at least four times, and the reported data are the average values with error bars indicating the standard deviation.

Figure 3 shows the results obtained with an NR-loaded PS-*b*-PNIPAM brush, plotting the fluorescence intensity normalized with the highest value versus time. First, we investigated the release kinetics at two temperatures, 20 and 40 °C, which are below and above the LCST of PNIPAM, respectively (Figure 3a). Although the overall diffusion rate of NR was very slow due to its hydrophobic nature, the thermosensitive solubility of the PNIPAM top layer clearly made a difference. The maximum achievable release of NR, based on the relative intensity, is significantly lower at 40 °C than that at 20 °C, and the release speed appears much faster at 20 °C than at 40 °C. The two curves could be well fitted with a simple exponential according to $I = I_{max}(1 - \exp^{t/\tau})$, where I is the fluorescence intensity, I_{max} the maximum value, and τ the characteristic time at which the release reaches 63% of the maximum value. Fitting the data yielded I_{max} = 0.99 and τ = 51 min for 20 °C and I_{max} = 0.77 and τ = 85 min for 40 °C. This difference in the release kinetics should originate from the thermoresponsive behavior of the PNIPAM top layer. At 40 °C, PNIPAM chains are in a collapsed state, which makes the molecular permeability of the brush low and slows the diffusion of NR molecules across the brush. By contrast, at 20 °C, PNIPAM chains are soluble, which opens the top layer of the brush and favors the release of NR. The water solubility switch of the PNIPAM brush was confirmed by the water contact angle measurements (Supporting Information) conducted at 20 and 40 °C. We note that the difference in the achievable release of NR cannot be caused by a temperature effect because the saturation solubility of NR in water should increase with increasing temperature. Thermo-responsive phase transitions of PS-*b*-PNIPAM and PDMA-*b*-PNIAM grafted surfaces were confirmed by contact angle measurements taken by switching the temperature between 20 and 40 °C (Supporting Information). The advancing contact angle of 17 ± 3° was obtained at 20 °C (T < LCST). In contrast, a contact angle of 62 ± 2° was obtained after increasing the solution temperature to 40 °C (T > LCST).

As expected, even in the closed state (at T > LCST) schematized in Figure 1, the outer layer of PNIPAM could not act as an impermeable cap preventing the release of dye molecules. PNIPAM chains in the collapsed state should still be hydrated to some extent and allow dye molecules to diffuse out of the brushes. With the used experimental setup (Figure2), the measured fluorescence intensity is determined by the concentration of the dye molecules solubilized in water outside the dialysis cap holding the substrate with grafted BCP brushes. Since NR is a hydrophobic dye, the flattened (maximum) intensity at a given temperature (Figure 3a) should be determined by its saturation concentration in equilibrium with dye molecules preferentially solubilized by the hydrophobic region of the BCP brush. At 40 °C (T > LCST), PNIPAM chains are more dehydrated, and the whole BCP brush is more hydrophobic than at 20 °C (T < LCST); consequently, more NR molecules should be partitioned in the PS-*b*-PNIPAM brush, resulting in less dye molecules released into the water at equilibrium. Therefore, as seen from the data fitting in Figure 3, collapsed PNIPAM chains on top not only have the effect of slowing down the release rate of NR, which is noticeable from the longer characteristic release time, but also have the effect of reducing the amount of dye molecules released into water at equilibrium, which is revealed by the lower flattened fluorescence intensity at 40 °C. The used experimental setup also accounts for the apparent release profile. When the substrate containing the BCP brush is immersed in water, dye molecules start to diffuse out of the brush; as its concentration in water is getting close to saturation, the diffusion slows down before flattening at equilibrium. The release profile is similar to that of the release of hydrophobic dyes loaded in BCP micelles in an LbL multilayer film immersed in aqueous solution.[19c]

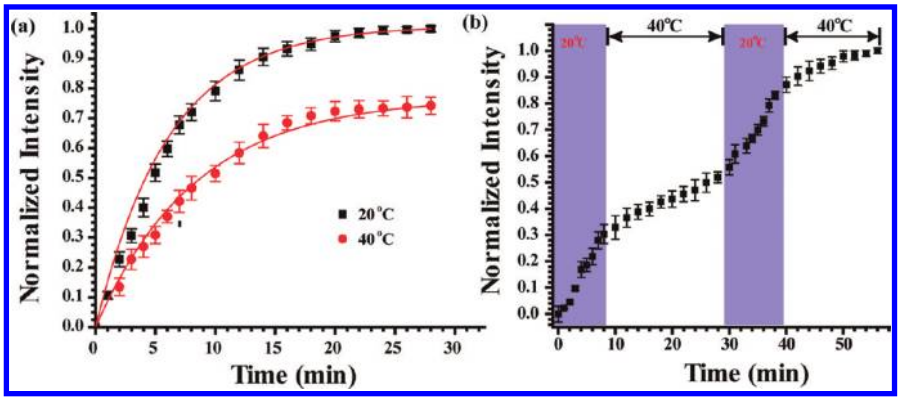

Figure 4. (a) Changes in normalized fluorescence emission intensity of PTS (λ_{ex} = 380 nm) over time showing the dye release kinetics from the PDMA-*b*-PNIPAM brush at two different temperatures. (b) Dye release profile recorded by switching the solution temperature between 20 and 40 °C.

Although the release of NR from the PS-*b*-PNIPAM brush cannot be stopped at T > LCST (40 °C), the significantly slowed kinetics and the reduced amount of released NR molecules make it possible to thermally switch the release of the dye by cycling the solution temperature below and above the LCST of PNIPAM. This control is demonstrated by the result presented in Figure 3b. In this experiment, the NR-loaded PS-*b*-PNIPAM brush was first immersed in water at 20 °C; the swollen top PNIPAM layer allowed the release of NR to proceed in a favorable condition, as is visible from the fast increase in the fluorescence intensity. After 40 min of dye release, the solution was quickly heated to 40 °C (i.e., within 1 min), and the release became much slower due to the closure of the PNIPAM layer. When the solution was cooled to 20 °C again, the faster release kinetics was recovered, and when heated to 40 °C for a second time, the release appeared to be slowed down again. Finally, when the solution was set at 20 °C, the maximum release, corresponding to the saturation concentration of NR in water, was achieved. Further switching of the solution temperature resulted in little change in the amount of released dye molecules. This ability to turn on and subsequently turn off (actually slow down) the dye release by switching the solution temperature makes these model systems highly attractive.

Next, we investigated the thermoresponsive release of the hydrophilic dye PTS from the PDMA-*b*-PNIPAM brush by carrying out the same experiments as described above. The results are shown in Figure 4. Basically, the same observations and analyses can be made as mentioned above, confirming our interpretation. A notable difference is that the hydrophilic nature of PTS makes its release into water much faster than that of NR. At both 20 and 40 °C, the release of PTS essentially reaches the maximum value within 30 min, but the soluble PNIPAM top layer at 20 °C still leads to a more effective and faster release of the dye than the collapsed PNIPAM at 40 °C (Figure 4a). Fitting the two curves with an exponential curve yielded I_{max} = 0.99 and τ = 6.11 min for 20 °C and I_{max} = 0.77 and τ = 8.3 min for 40 °C. Although not as effectively as for NR-loaded PS-*b*-PNIPAM, the difference in the kinetics for the two temperatures could be used to thermally switch the rate of dye release through the PDMA-*b*-PNIPAM brush through the closure and opening of PNIPAM chains, as demonstrated by the repeatable effect upon cycling of the solution temperature between 20 and 40 °C (Figure 4b).

The above results demonstrate that using appropriate engineering of the surface-grafted diblock copolymer brush, both hydrophobic and hydrophilic dyes can be entrapped by the brush, and their release into water can be thermosensitive or thermally controlled to some extent through the thermal phase transition of the BCP brush. The LCST of the PNIPAM top layer leads to faster release at lower temperatures (below LCST) and slower release at higher temperatures (above LCST). If the top layer block is a polymer having an upper critical solution temperature (UCST), the opposite trend should be expected. Therefore, in principle, through thermally induced closure and opening of the brush top layer, temperature change can be utilized as a trigger to repeatedly stop or start the release of loaded compounds on demand. However, the results in Figures 3 and 4 also point out that even with the top layer of the BCP brush in the collapsed state (T > LCST or T < UCST), it would be challenging to completely prevent the release of the dye. These brushes may be interesting for applications where a control of the release rate is mostly desired.

3.3. Photosensitive BCP Brush and Dye Release. As mentioned above, the BCP brush design for stimuli-sensitive release is general since the solubility switch of the top brush layer can also be triggered by other signals such as exposure to light and pH change. To investigate the possible photocontrollable release from the BCP brush, we synthesized surface-grafted PS-*b*-PNBA (Figure 1). The photoinduced removal of *o*-nitrobenzyl has been used in various polymer systems such as LbL films[28] and BCP micelles,[29] to switch the hydrophilic−hydrophobic balance and obtain photocontrolled release. With the PS-*b*-PNBA brush in water, as the photocleavage proceeds converting hydrophobic *o*-nitrobenzyl methacrylate to hydrophilic methacrylic acid (MA), the PNBA top layer should gradually increase its polarity before becoming hydrophilic PMA upon complete photocleavage. This photoinduced polarity (and solubility) change of the top brush layer should impact the release kinetics of loaded NR.

First, we carried out experiments to confirm the effective removal of *o*-nitrobenzyl groups from the PS-*b*-PNBA brush immersed in water under UV irradiation. The photocleavage by irradiation at 360 nm (10 mW/cm^2) was monitored by observing the changes in the absorption of the chromophore. Figure 5a shows the UV−vis spectra of the PS-*b*-PNBA brush on a quartz slide as a function of UV irradiation time. The absorbance at 360 nm, corresponding to the 4,5-dimethoxy-2-nitrobenzyl group, decreased over irradiation time and almost disappeared after 30 min, indicating the complete photochemical reaction. After UV irradiation, the brush was washed with water and used for contact angle analyses. The inset of Figure 5a shows that the water contact angles decreased from 90 ± 4° before UV

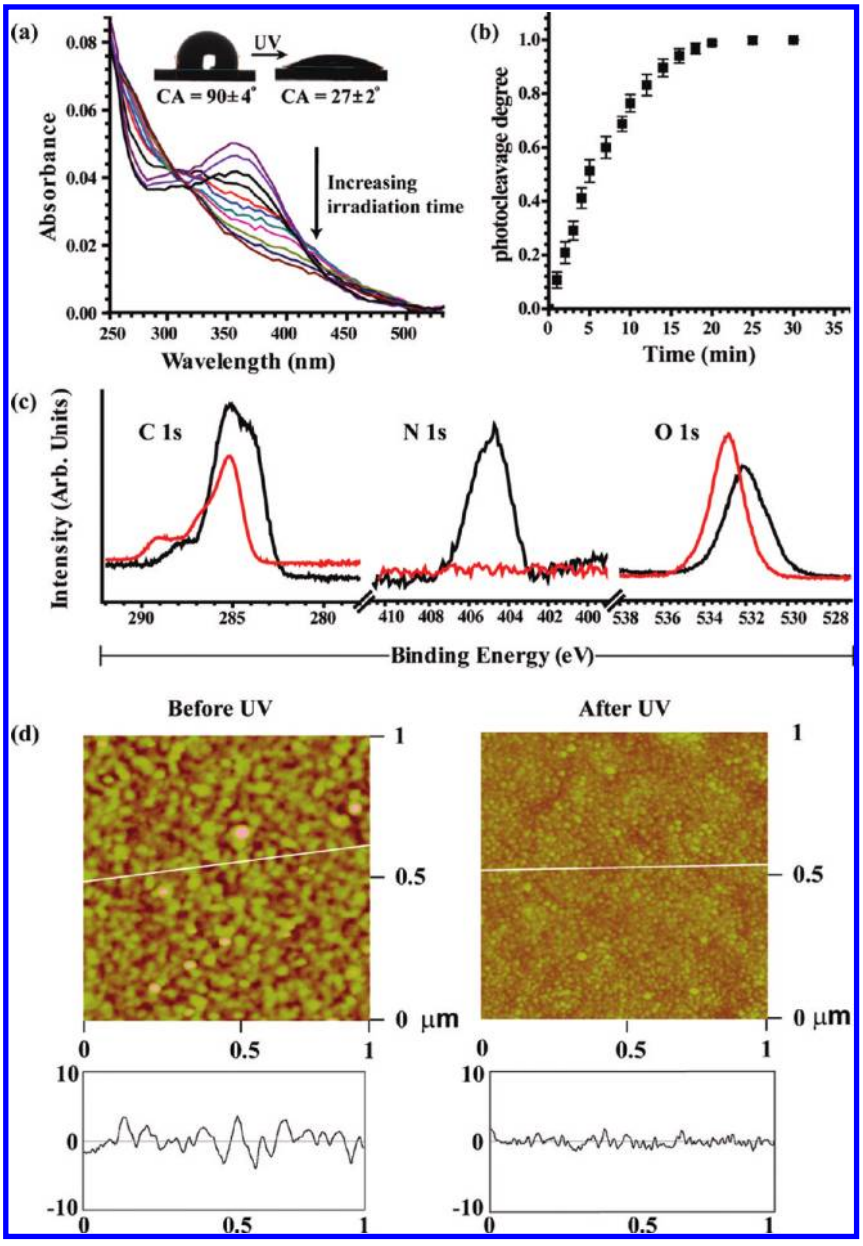

Figure 5. (a) UV−vis spectra of the PS-*b*-PNBA brush on quartz under different times of UV irradiation (360 nm, 10 mW/cm^2) with the inset showing the change in the water contact angle after complete photocleavage of *o*-nitrobenzyl; (b) photocleavage degree vs UV irradiation time; (c) high-resolution C1s, N1s, and O1s XPS spectra of the PS-*b*-PNBA brush before (black curve) and after (red curve) UV irradiation; and (d) AFM height images of the PS-*b*-PNBA brush before and after UV irradiation. The height profiles correspond to the white lines on the corresponding image.

irradiation to 27 ± 2° after 30 min UV exposure, confirming the photoinduced cleavage of the *o*-nitrobenzyl groups and the resulting hydrophobic−hydrophilic switching of the brush top layer. From the absorption spectra, the photocleavage degree can be calculated from $1 - A_t / A_0$, where A_0 and A_t are the initial absorbance and the absorbance after irradiation time t at 360 nm, respectively. The plot of photocleavage degree as a function of irradiation time is shown in Figure 5b. The complete photocleavage on the PNBA brush was also confirmed by XPS analyses as shown in Figure 5c. The C1s signal of the PNBA brush consists of an aromatic carbon peak at the binding energy of 283.5 eV, which disappeared after UV irradiation. The photoelectron peak of the N1s for the $-NO_2$ group at 405 eV was also observed only on the PNBA surface before UV irradiation; while the peak at 532.7 eV for O1s shifted to lower binding energy after UV irradiation due to the cleavage of the *o*-nitobenzyl group to form the corresponding acrylic acid. The AFM height images in Figure 5d show changes in the surface morphology before and after UV irradiation; the brush surface appears to be smoother after the photocleavage of *o*-nitrobenzyl groups.

As shown in Figure 5, the photocleavage degree based on the decrease of the absorption of *o*-nitrobenzyl at 360 nm could be precisely controlled by the UV irradiation time. We thus investigated the effect of increasing the photocleavage degree of the top PNBA brush on the release kinetics of NR. The results are shown in Figure 6a. We emphasize that each curve was obtained with a separate sample of the PS-*b*-PNBA brush and was exposed to UV light to obtain a given photocleavage degree, and all release

dx.doi.org/10.1021/ma2010102 |*Macromolecules* 2011, 44, 7385–7393

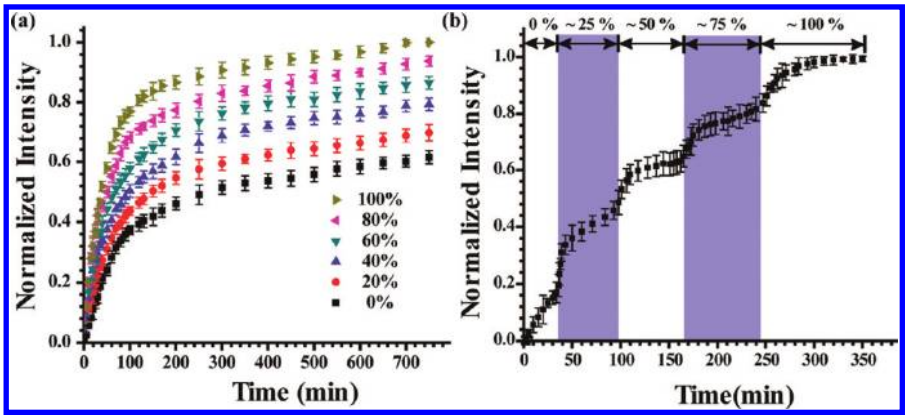

Figure 6. (a) Changes in normalized fluorescence emission intensity of Nile Red (λ_{ex} = 640 nm) over time showing the dye release kinetics from the PS-*b*-PNBA brush subjected to different photocleavage degrees of *o*-nitrobenzyl groups. (b) Dye release profile recorded upon stepwise increase of the photocleavage degree.

measurements were performed under the same conditions (at room temperature). The results show that as the photocleavage degree increases, which increases the amount of hydrophilic methacrylic acid groups in the top brush layer, the amount of NR released into water increases constantly. Being increasingly hydrophilic for the top brush layer means more and more water molecules absorbed or surrounding the brush, which makes the diffusion of hydrophobic NR out of the brush easier. Understandably, the largest difference is between the initial PS-*b*-PNBA brush without photocleavage and the brush subjected to complete photoreaction, i.e., the PS-*b*-PMA brush. For instance, after 100 min, the amount of NR released from the latter is double that released from the former. Fitting these two curves yielded a characteristic release time τ = 90 min for PS-*b*-PMA and τ = 115 min for PS-*b*-PNBA. These results demonstrate that the photoinduced switching from the hydrophobic PNBA top brush to the hydrophilic PMA results in a more important and faster release of NR from the BCP brush. A feature of interest of the BCP brush capable of photosensitive release is that the precisely controllable photocleavage degree provides a convenient means to tune the release kinetics.

The phototunable release kinetics based on controlling the photocleavage degree of the top PNBA brush offers the possibility to design complex photocontrollable release profiles. We demonstrated this with the experiment described in Figure 6b. In this case, the NR-loaded PS-*b*-PNBA brush grafted on a quartz slide was immersed in water at room temperature using the setup in Figure 2b; the release of NR was monitored by the measured fluorescence intensity. After a selected duration (35 min), UV irradiation was applied directly on the BCP brush from the top of the dialysis cap (using a fiber optic light guide) for the time required to obtain 25% photocleavage (~2 min), and immediately after turning off the UV irradiation, the fluorescence emission measurement continued. It can be seen that the partial photocleavage increased the amount of released NR quickly before the release rate was stabilized over time. When UV irradiation was applied again to increase the photocleavage degree to 50%, the amount of released dye molecules jumped again. A similar effect was observed when the photocleavage degree was further increased to 75 and 100%; that is, every irradiation (short time) triggered an increased amount of dye released into water as a result of the light-controllable hydrophilicity of the top brush layer. This stepped profile of the dye release progress is a demonstration of the temporal control by using light as a trigger for BCP brushes. It is easy to conceive that with such a photosensitive BCP brush grafted on a large substrate, a laser light can also offer the appealing spatial control of the release by activating the photoreaction in selected areas.

In the present study, the photocleavage of *o*-nitrobenzyl of the PS-*b*-PNBA brush is not a reversible photochemical reaction. Obviously, it cannot be used to achieve the reversible closure and opening of the top brush layer by light as depicted in Figure 1. Such a reversible photocontrol in principle is achievable by using a reversible photoreaction that switches the top layer between the hydrophobic and hydrophilic states. The reversible spiropyran-merocyanine can possibly be explored for this purpose. However, as demonstrated above, the irreversible photocleavage reaction offers the unique possibility to control the hydrophilicity of the top brush layer and thus to precisely tune the release kinetics. In designing the photosensitive PS-*b*-PNBA brush, we also had in mind that complete removal of the photolabile groups resulted in the pH-sensitive PS-*b*-PMA brush with which another trigger, pH change, could be investigated.

3.4. PH-Sensitive BCP Brush and Dye Release. Finally, pH-responsive dye release was studied using the PS-*b*-PMA brush resulting from the complete removal of *o*-nitrobenzyl groups from the PS-*b*-PNBA brush. The pH-induced switch of the top PMA layer between the collapsed and swollen states was first confirmed by the surface wettability measurements of the PS-*b*-PMA brush subjected to different pH values in aqueous solution (using HCl and NaOH to adjust the pH value). As shown in Figure 7a, upon pH increase, the water contact angle indicates a transition from hydrophobic PMA with protonated carboxylic acid groups to hydrophilic PMA with ionized acid groups around pH 5, which is consistent with the range of reported values of pK_a (6.2−7 in polymer brushes).[25] In view of these results, we carried out the fluorescence measurements to monitor the release kinetics of NR from the silicon-grafted PS-*b*-PMA brush immersed in aqueous solutions having pH values between 2 and 7, a range in which the brush exhibited good stability. The experiment at each pH was performed using a separate sample. Figure 7b shows two examples of the data obtained at pH 7 and pH 3. Again, the swollen top brush layer at pH 7 allowed more NR molecules to be released into the solution with a faster rate than the collapsed layer at pH 3. In this case, the data could not be well fitted with a simple exponential. Nevertheless, fitting

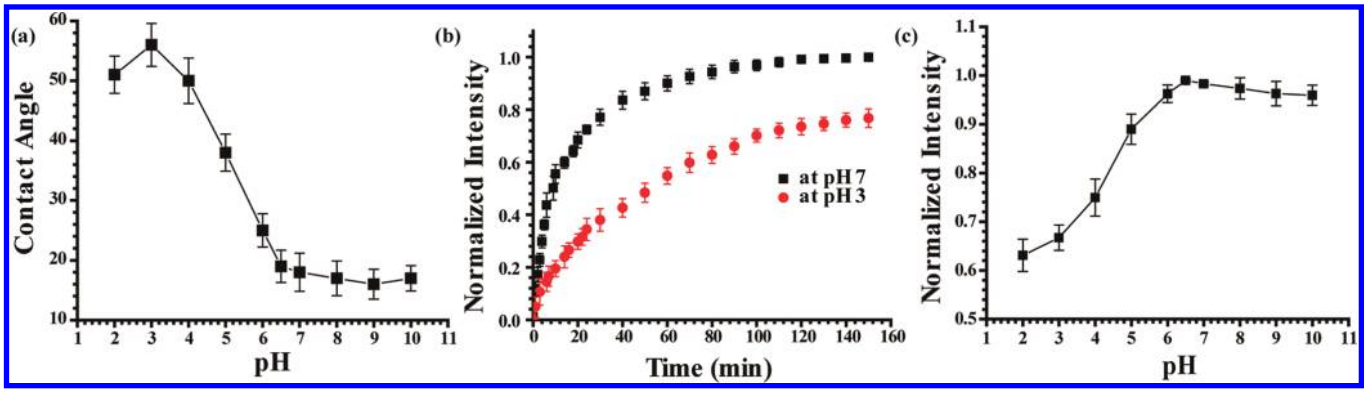

Figure 7. (a) Advancing water contact angle of the PS-b-PMA surface as a function of pH. (b) Changes in normalized fluorescence emission intensity of Nile Red (λ_{ex} = 640 nm) over time showing the dye release kinetics from PS-b-PMA at two different pH values. (c) Maximum achievable amount of dye release as a function of pH.

was performed to have a qualitative magnitude for comparison and the results were I_{max} = 0.98 and τ = 18 min for pH 7 and I_{max} = 0.81 and τ = 54 min for pH 3. In Figure 7c, data obtained at all investigated pH values are summarized by plotting the maximum achievable amount of dye release I_{max} as a function of pH (data obtained after about 1 h dye release). The curve appears to be inversely correlated to the plot of water contact angle vs pH (Figure 7a), suggesting that the release of NR is mainly determined by the hydrophilicity of the top brush layer of PMA.

The above results clearly demonstrate that the release of hydrophobic dyes like NR from the PS-*b*-PMA brush is sensitive to the pH of the releasing solution. The amount of released NR increased with increasing pH. Therefore, the pH effect on a carboxylic acid polymer brush provides the controlled release of loaded guest molecules because the degree of dissociation of acid groups varies reversibly with the pH change of the medium. In an acidic medium (pH 3), the carboxylic acid groups are fully protonated, whereas the degree of dissociation becomes higher with increasing the pH. Finally, we note that since the pH-induced swelling and collapse of PMA is reversible, the pH change could be used to reduce the swelling of a polymer brush, thereby enhancing the flexibility in tuning the dye release.

A couple of final thoughts are worth being mentioned. First, at this point, we do not have direct evidence that the BCP brushes formed a layered structure as depicted in Figure 1. However, in all cases, without ruling out the possibility of chain mixing, the clearly observed stimuli-responsiveness implies the segregation of the two blocks and that it was mainly the second block constituting the BCP brush surface, while the first block, which is nonstimuli-responsive, formed the inner region. Second, although the present study shows that it is possible to use a stimuli-responsive block to mediate the release of loaded dyes, the extent of the control is limited. The reason is that even in the dehydrated (hydrophobic) state, the top layer still allows release to occur. In future studies, it would be of interest to develop top layers that exhibit a large difference in permeability between the extended and collapsed states in response to stimuli. Other molecular variables, such as the relative lengths of the two blocks, which should determine the thicknesses of the inner and outer layers, could also affect the performance of controlled release using BCP brushes.

4. CONCLUSIONS

We presented a general design of diblock copolymer brushes that can be used as stimuli-sensitive release systems. Being grafted from the surface of a substrate, while the first block (inner layer) can either be hydrophobic or hydrophilic, the water solubility of the second block (outer layer) can be switched, or changed, in response to a temperature or pH change, or to exposure to UV light. The release kinetics of encapsulated dyes is controlled by the solubility of the outer layer between collapsed and extended states. To investigate this approach, we synthesized diblock copolymer brushes of PS-*b*-PNIPAM, PDMA-*b*-PNIPAM, and PS-*b*-PNBA using sequential ATRP with a bromoisobutyrate initiator self-assembled monolayer. These BCP brushes were characterized by XPS, water contact angle, and AFM. The PS-*b*-PNIPAM and PDMA-*b*-PNIPAM brush assemblies exhibited reversible swelling transitions and were capable of controlling the release rate of an incorporated hydrophobic or hydrophilic dye in response to temperature variations due to the LCST of the outer PNIPAM layer. In the case of PS-*b*-PNBA, selective cleavage of *o*-nitrobenzyl in the brush could be manipulated by UV light irradiation, and by converting the hydrophobic *o*-nitrobenzyl methacrylate into hydrophilic methacrylic acid (MA), the diblock brush exhibited photoregulated hydrophobic dye release from the surface. Moreover, after full photocleavage, the resultant PS-*b*-PMA diblock brush became pH-sensitive. Control of the dye released from the brush by pH changes was demonstrated by defining the swelling and collapse transitions of the outer PMA block. These newly developed thermo-, light-, and pH-activated diblock copolymer brushes could be of interest for applications where a stimuli-sensitive release of guest molecules from the substrate surface is required.

■ ASSOCIATED CONTENT

Supporting Information. Block copolymer synthesis details, XPS data, AFM images, contact angles of brushes, and details of release studies. This material is available free of charge via the Internet at http://pubs.acs.org.

■ AUTHOR INFORMATION

Corresponding Author

*E-mail: yves.dory@usherbrooke.ca (Y.L.D), martin.lepage@usherbrooke.ca (M.L.), yue.zhao@usherbrooke.ca (Y.Z.).

■ ACKNOWLEDGMENT

We acknowledge the financial support of Le Fonds Quebecois de la Recherche sur la Nature et les Technologies of Quebec (FQRNT) and the Natural Sciences and Engineering Research Council of Canada (NSERC). We also thank Mrs. Sonia Blais and Xia Tong for their help with the XPS and AFM measurements and analyses, respectively. M.L. is a member of the Canada Research Chair in Magnetic Resonance Imaging and of the FRSQ-funded Centre de recherche clinique Étienne−Le Bel. Y.L.D. and Y.Z. are members of the FQRNT-funded Center for Self-Assembled Chemical Structures (CSACS).

■ REFERENCES

(1) (a) Uhrich, K. E.; Cannizzaro, S. M.; Langer, R. S.; Shakesheff, K. M. *Chem. Rev.* **1999**, *99*, 3181. (b) Kataoka, K.; Harada, A.; Nagasaki, Y. *Adv. Drug Delivery Rev.* **2001**, *47*, 113.

(2) Harris, J. M.; Chess, R. B. *Nat. Rev. Drug Discovery* **2003**, *2*, 214.

(3) (a) Bertin, P. A.; Smith, D. D.; Nguyen, S. T. *Chem. Commun.* **2005**, 3793. (b) Duncan, R. *Nat. Rev. Drug Discovery* **2003**, *2*, 347. (c) Khandare, J.; Minko, T. *Prog. Polym. Sci.* **2006**, *31*, 359.

(4) (a) Bae, Y.; Fukushima, S.; Harada, A.; Kataoka, K. *Angew. Chem., Int. Ed.* **2003**, *42*, 4640. (b) Nishiyama, N.; Kataoka, K. *Adv. Polym. Sci.* **2006**, *193*, 67. (c) Sant, V. P.; Smith, D.; Leroux, J.-C. *J. Controlled Release* **2004**, *97*, 301. (d) Jiang, J.; Tong, X.; Zhao, Y. *J. Am. Chem. Soc.* **2005**, *127*, 8290. (e) Soppimath, K. S.; Tan, D. C.-W.; Yang, Y.-Y. *Adv. Mater.* **2005**, *17*, 318. (f) Sheihet, L.; Dubin, R. A.; Devore, D.; Kohn, J. *Biomacromolecules* **2005**, *6*, 2726. (g) Pelletier, M.; Babin, J.; Tremblay, L.; Zhao, Y. *Langmuir* **2008**, *24*, 12664.

(5) (a) Discher, D. E.; Eisenberg, A. *Science* **2009**, *297*, 967. (b) Wu, J.; Eisenberg, A. *J. Am. Chem. Soc.* **2006**, *28*, 2880. (c) Du, J.; O'Reilly, R. K. *Soft Matter* **2009**, *5*, 3544. (d) He, J.; Tong, X.; Tremblay, L.; Zhao, Y. *Macromolecules* **2009**, *42*, 7267. (e) Tong, X.; Wang, G.; Soldera, A.; Zhao, Y. *J. Phys. Chem. B* **2005**, *109*, 20281. (f) He, J.; Tong, X.; Zhao, Y. *Macromolecules* **2009**, *42*, 4845.

(6) (a) Gillies, E. R.; Jonsson, T. B.; Fréchet, J. M. *J. Am. Chem. Soc.* **2004**, *126*, 11936. (b) Boas, U.; Heegaard, P. M. H. *Chem. Soc. Rev.* **2004**, *33*, 43.

(7) (a) Zelikin, A. N. *ACS Nano* **2010**, *4*, 2494. (b) Kim, Y. S.; Smith, R. C.; Poon, Z.; Hammond, P. T. *Langmuir* **2009**, *25*, 14086.

(8) (a) Stuart, M. A. C.; Huck, W. T. S.; Genzer, J.; Muller, M.; Ober, C.; Stamm, M.; Sukhorukov, G. B.; Szleifer, I.; Tsukruk, W.; Urban, M.; Winnik, F.; Zauscher, S.; Luzinov, I.; Minko, S. *Nat. Mater.* **2010**, *9*, 101. (b) Tokarev, I.; Minko, S. *Adv. Mater.* **2010**, *22*, 3446.

(9) (a) Miyata, T.; Asami, N.; Uragami, T. *Nature* **1999**, *399*, 766. (b) Bromberg, L. E.; Ron, E. S. *Adv. Drug Delivery Rev.* **1998**, *31*, 197.

(10) (a) Ichimura, K. *Chem. Rev.* **2000**, *100*, 1847. (b) Advincula, R.; Park, M.-K.; Baba, A.; Kaneko, F. *Langmuir* **2003**, *19*, 654.

(11) (a) Hiller, J.; Rubner, M. F. *Macromolecules* **2003**, *36*, 4078. (b) Hiller, J.; Mendelsohn, J. D.; Rubner, M. F. *Nat. Mater.* **2002**, *1*, 59.

(12) Chang, D. P.; Dolbow, J. E.; Zauscher, S. *Langmuir* **2007**, *23*, 250.

(13) (a) Park, M. K.; Deng, S.; Advincula, R. C. *J. Am. Chem. Soc.* **2004**, *126*, 13723. (b) Balachandra, A. M.; Dai, J.; Bruening, M. L. *Macromolecules* **2002**, *35*, 3171. (c) Kumar, S. K.; Hong, J.-D. *Langmuir* **2008**, *24*, 4190. (d) Kumar, S. K.; Pennakalathil, J.; Kim, T.-H.; Kim, K.; Park, J.-K.; Hong, J.-D. *Langmuir* **2009**, *25*, 1767.

(14) (a) Decher, G. *Science* **1997**, *277*, 1232. (b) Such, G. K.; Johnston, A. P. R.; Caruso, F. *Chem. Soc. Rev.* **2011**, *40*, 19. (c) Sukhorukov, G. B.; Brumen, M.; Donath, E.; Möhwald, H. *J. Phys. Chem. B* **1999**, *103*, 6434. (d) Becker, A. L.; Johnston, A. P. R.; Caruso, F. *Small* **2010**, *6*, 1836. (e) Zhang, Y. J.; Yang, S. G.; Guan, Y.; Cao, W. X.; Xu, J. *Macromolecule* **2003**, *36*, 4238.

(15) (a) Hammond, P. T. *Nat. Mater.* **2010**, *9*, 292. (b) Kim, B. S.; Park, S. W.; Hammond, P. T. *ACS Nano* **2008**, *2*, 386. (c) Smith, R.; Riollano, M.; Leung, A.; Hammond, P. T. *Angew. Chem., Int. Ed.* **2009**, *48*, 8974.

(16) (a) Caruso, F.; Quinn, J. F. *Langmuir* **2004**, *20*, 20. (b) Onda, M.; Ariga, K.; Kunitake, T. *J. Biosci. Bioeng.* **1999**, *87*, 69. (b) Nolan, C. M.; Serpe, M. J.; Lyon, L. A. *Biomacromolecules* **2004**, *5*, 1940. (c) Serpe, M. J.; Yarmey, K. A.; Nolan, C. M.; Lyon, L. A. *Biomacromolecules* **2005**, *6*, 408.

(17) (a) Wood, K. C.; Boedicker, J. Q.; Lynn, D. M.; Hammond, P. T. *Langmuir* **2005**, *21*, 1603. (b) Thierry, B.; Tkaczyk, C.; Kujawa, P.; Winnik, F. M.; Bilodeau, L.; Tabrizian, M. *J. Am. Chem. Soc.* **2005**, *127*, 1626. (c) Kim, B. S.; Lee, H. L.; Min, Y. H.; Poon, Z.; Hammond., P. T. *Chem. Commun.* **2009**, 4194. (d) Sukhishvili, S. A.; Granick, S. *Macromolecules* **2002**, *35*, 301. (e) Sukhishvili, S. A.; Granick, S. *J. Am. Chem. Soc.* **2000**, *122*, 9550.

(18) Thierry, B.; Kujawa, P.; Tkaczyk, C.; Winnik, F. M.; Bilodeau, L.; Tabrizian, M. *J. Am. Chem. Soc.* **2005**, *127*, 1626.

(19) (a) Qi, B.; Tong, X.; Zhao, Y. *Macromolecules* **2006**, *39*, 5714. (b) Zhao, Y.; Bertrand, J.; Tong, X.; Zhao, Y. *Langmuir* **2009**, *25*, 13151. (c) Ma, N.; Zhang, H. Y.; Song, B.; Wang, Z. Q.; Zhang, X. *Chem. Mater.* **2005**, *17*, 5065. (d) Ma, N.; Wang, Y.; Wang, Z.; Zhang, X. *Langmuir* **2006**, *22*, 3906.

(20) (a) Advincula, R. C., Brittain, W. J., Caster, K. C., Rühe, J., Eds.; *Polymer Brushes: Synthesis, Characterization, Application*; Wiley-VCH: New York, 2004; p 273. (b) Barbey, R.; Lavanant, L.; Paripovic, D.; Schower, N.; Sugnaux, C.; Tugulu, S.; Klok, H. A. *Chem. Rev.* **2009**, *109*, 5437. (c) Edmondson, S.; Osborne, V. L.; Huck, W. T. S. *Chem. Soc. Rev.* **2004**, *33*, 14.

(21) (a) Matyjaszewski, K.; Xia, J. *Chem. Rev.* **2001**, *101*, 2921. (b) Patten, T. E.; Xia, J.; Abernathy, T.; Matyjaszewski, K. *Science* **1996**, *272*, 866. (c) Ejaz, M.; Yamamoto, S.; Ohno, K.; Tsujii, Y.; Fukuda, T. *Macromolecules* **1998**, *31*, 5934. (d) Edmondson, S.; Osborne, V. L.; Huck, W. T. S. *Chem. Soc. Rev.* **2004**, *33*, 14.

(22) (a) Ueno, K.; Inaba, A.; Kondoh, M.; Watanabe, M. *Langmuir* **2008**, *24*, 5253. (b) Zou, Y.; Ying, P.; Yeh, J.; Rossi, N. A. A.; Brooks, D. E.; Kizhakkedathu, J. N. *Biomacromolecules* **2010**, *11*, 284. (c) Zhou, F.; Shu, W. M.; Welland, M. E.; Huck, W. T. S. *J. Am. Chem. Soc.* **2006**, *128*, 5326. (d) Chen, T.; Chang, D. P.; Liu, T.; Desikan, R.; Datar, R.; Thundat, T.; Berger, R.; Zauscher, S. *J. Mater. Chem.* **2010**, *20*, 3391. (e) Lokuge, I.; Wang, X.; Bohn, P. W. *Langmuir* **2007**, *23*, 305.

(23) (a) Okano, T. In *Adv. Polym. Sci., Responsive Gels; Volume Transition II*; Dusek, K., Ed.; Springer: Berlin, Germany, 1993; p 179. (b) Park, T. G.; Hoffman, A. S. *Macromolecules* **1993**, *26*, 5045. (c) Takei, Y. G.; Aoki, T.; Sanui, K.; Ogata, N.; Sakurai, Y.; Okano, T. *Macromolecules* **1994**, *27*, 6163. (d) Jones, D. M.; Smith, J. R.; Huck, W. T. S.; Alexander, C. *Adv. Mater.* **2002**, *14*, 1130.

(24) (a) Aujard, I.; Benbrahim, C.; Gouget, M.; Ruel, O.; Baudin, J.-B.; Neveu, P.; Jullien, L. *Chem.—Eur. J.* **2006**, *12*, 6865. (b) Piggott, M.; Karuso, P. *Tetrahedron Lett.* **2005**, *46*, 8241. (c) Whitehouse, L.; Savinov, S. N.; Austin, D. J. *Tetrahedron Lett.* **1997**, *38*, 7851.

(25) (a) Izumrudov, V. A.; Kharlampieva, E.; Sukhishvili, S. A. *Biomacromolecules* **2005**, *6*, 1782. (b) Dong, R.; Lindau, M.; Ober, C. K. *Langmuir* **2009**, *25*, 4774. (c) Santonicola, M. G.; de Groot, G. W.; Memesa, M.; Meszynska, A.; Vancso, G. J. *Langmuir* **2010**, *26*, 17513. (d) Schuwer, N.; Klok, H. A. *Langmuir* **2011**, *27*, 4789.

(26) (a) Ell, J. R.; Mulder, D. E.; Faller, R.; Patten, T. E.; Kuhl, T. L. *Macromolecules* **2009**, *42*, 9523. (b) Jones, D. M.; Smith, J. R.; Huck, W. T. S.; Alexander, C. *Adv. Mater.* **2002**, *14*, 1130. (c) Kumar, S.; Ito, T.; Yanagihara, Y.; Oaki, Y.; Nishimura, T.; Kato, T. *CrystEngComm* **2010**, *12*, 2021. (d) Brown, A. A.; Azzaroni, O.; Huck, W. T. S. *Langmuir* **2009**, *25*, 1744.

(27) (a) Matyjaszewski, K.; Miller, P. J.; Shukla, N.; Immaraporn, B.; Gelman, A.; Luokala, B. B.; Siclovan, T. M.; Kickelbick, G.; Vallant, T.; Hoffmann, H.; Pakula, T. *Macromolecules* **1999**, *32*, 8716. (b) Zhao, B.; Brittain, W. J. *J. Am. Chem. Soc.* **1999**, *121*, 3557.

(28) (a) Dai, J.; Balachandra, A. M.; Lee, J. I.; Bruening, M. L. *Macromolecule* **2002**, *35*, 3164. (b) Jensen, A. W.; Desai, N. K.; Maru, B. S.; Mohanty, D. K. *Macromolecules* **2004**, *37*, 4196.

(29) (a) Jiang, J.; Tong, X.; Morris, D.; Zhao, Y. *Macromolecules* **2006**, *39*, 4633. (b) Han, D.; Tong, X.; Zhao, Y. *Macromolecules* **2011**, *44*, 437.